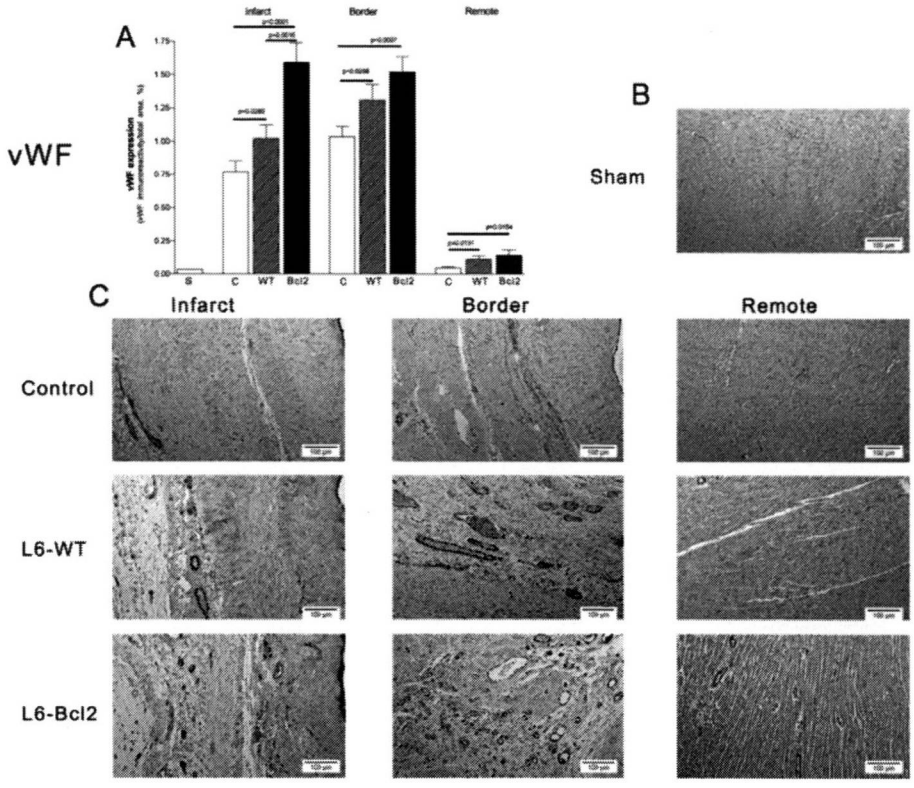
vWF
A
Infarct
Border
Remote
S
C
WT
Bcl2
B
Sham
C
Infarct
Border
Remote
Control
L6-WT
L6-Bcl2

Figure 4:

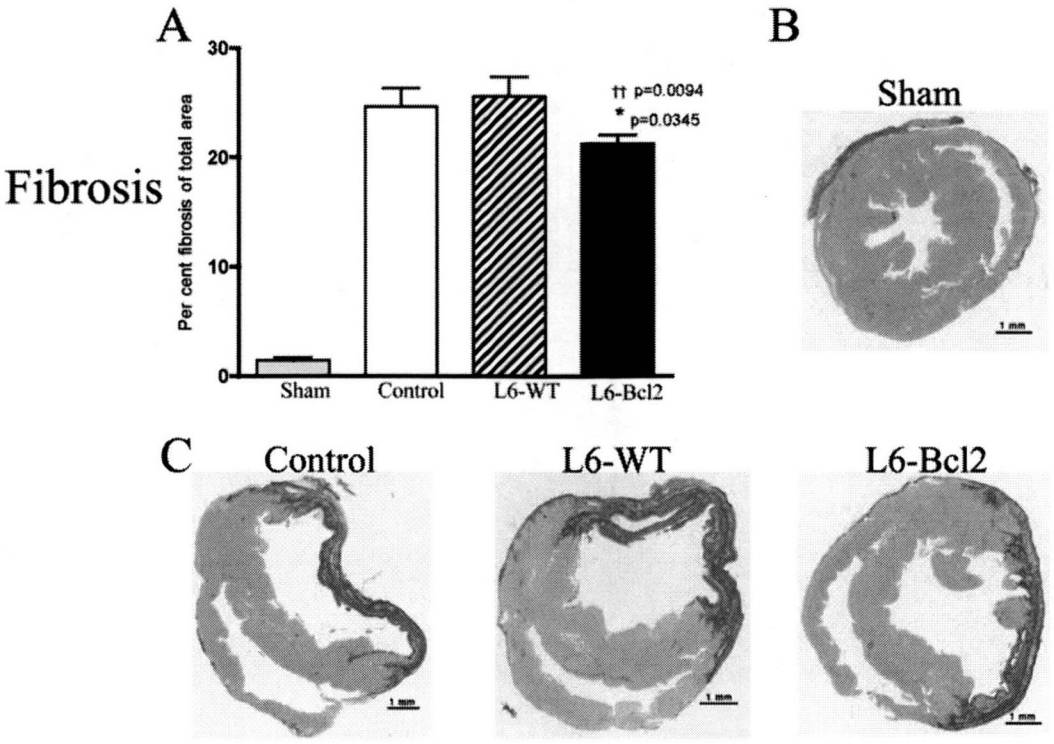
A
Fibrosis
Per cent fibrosis of total area
30
20
10
0
Sham
Control
L6-WT
L6-Bcl2
†† p=0.0094
* p=0.0345
B
Sham
1 mm
C
Control
L6-WT
L6-Bcl2
1 mm
1 mm
1 mm

Figure 5:

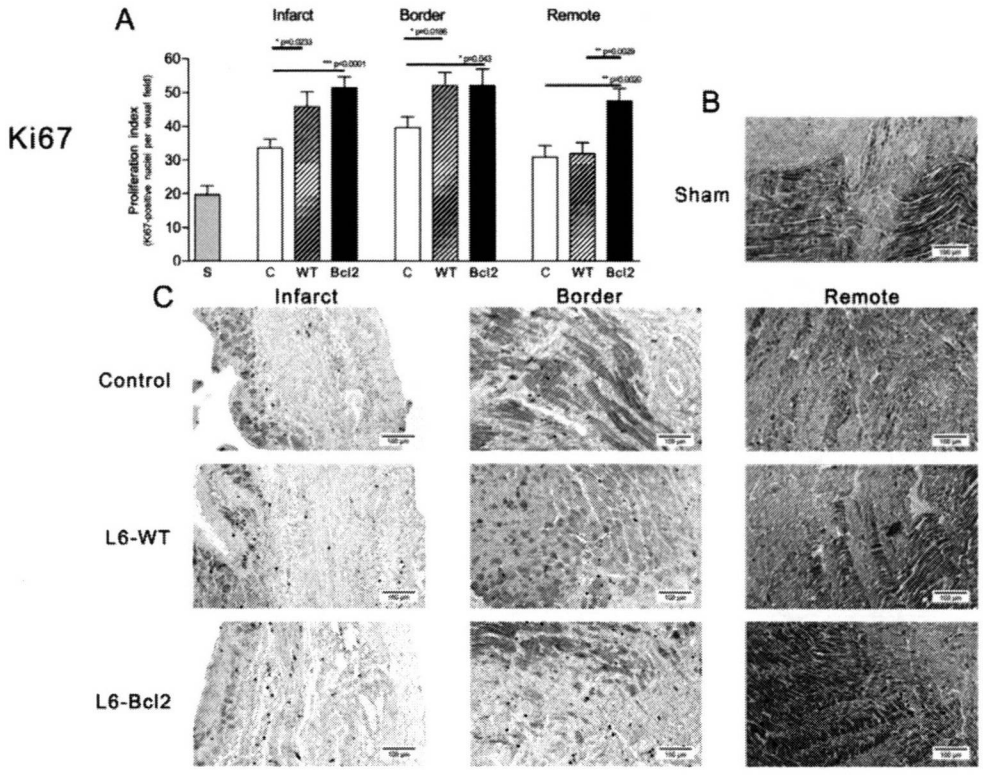
Ki67
A
Infarct
Border
Remote
Proliferation index
(Ki67-positive nuclei per visual field)
60
50
40
30
20
10
0
S
C
WT
Bcl2
C
WT
Bcl2
C
WT
Bcl2
B
Sham
C
Infarct
Border
Remote
Control
L6-WT
L6-Bcl2

Figure 6:

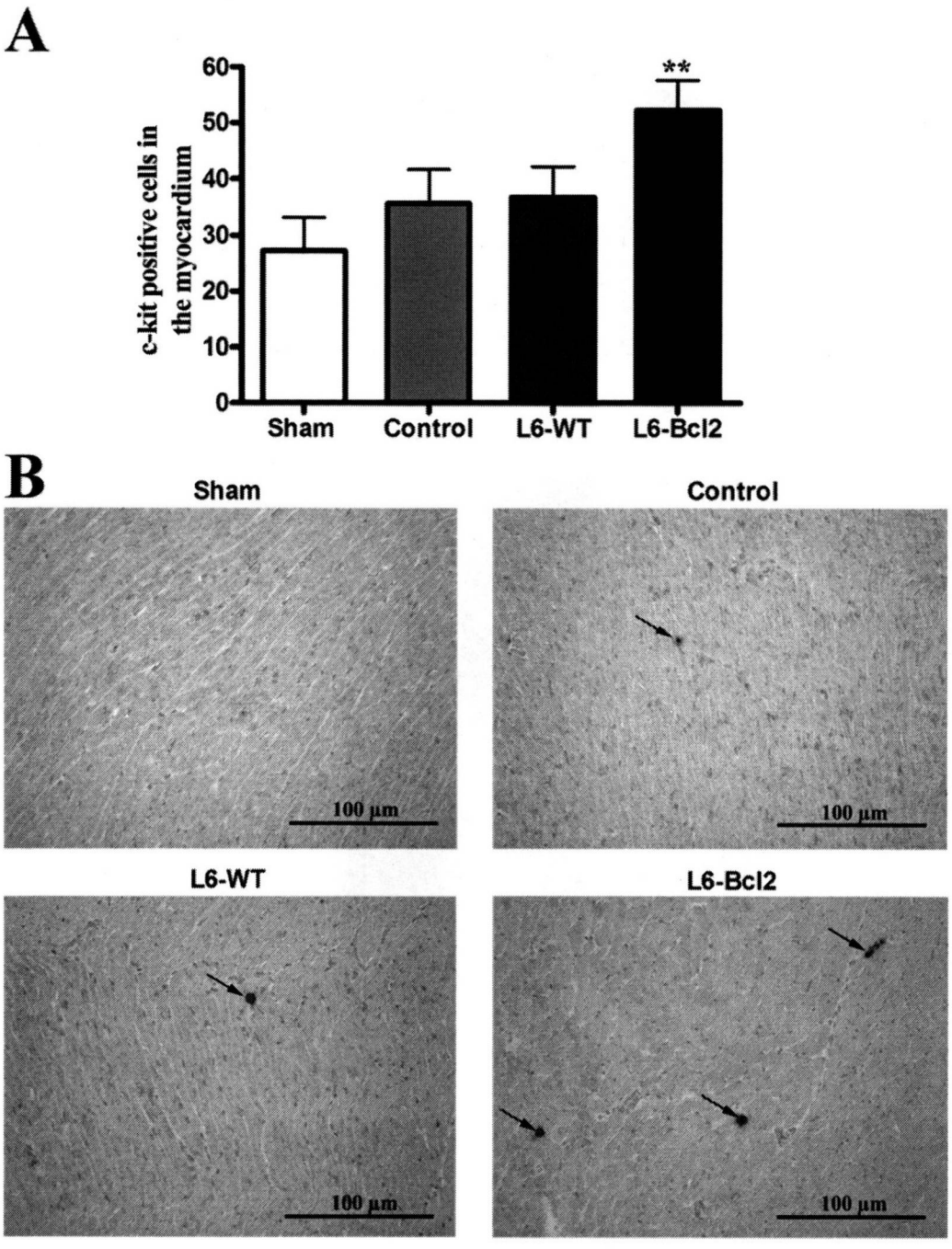
A
c-kit positive cells in the myocardium
60
50
40
30
20
10
0
**
Sham
Control
L6-WT
L6-Bcl2
B
Sham
Control
100 μm
100 μm
L6-WT
L6-Bcl2
100 μm
100 μm

Figure 7:

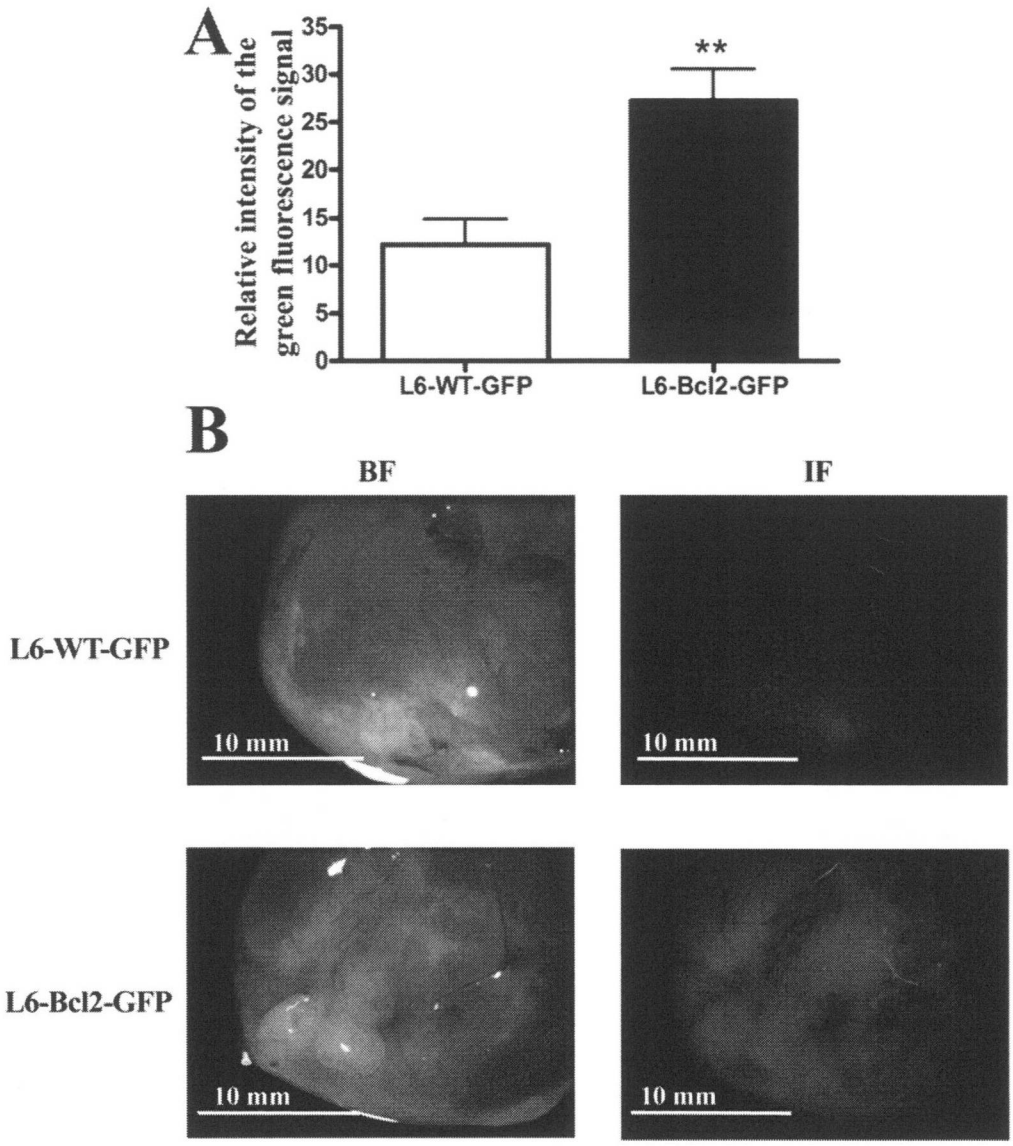
A
Relative intensity of the green fluorescence signal
35
30
25
20
15
10
5
0
**
L6-WT-GFP
L6-Bcl2-GFP
B
BF
IF
L6-WT-GFP
L6-Bcl2-GFP
10 mm
10 mm
10 mm
10 mm

Figure 8:

ELSEVIER

European Journal of Cardio-thoracic Surgery xxx (2010) xxx–xxx

EUROPEAN JOURNAL OF CARDIO-THORACIC SURGERY

www.elsevier.com/locate/ejcts

Engineering a novel three-dimensional contractile myocardial patch with cell sheets and decellularised matrix☆,☆☆

Hiroki Hata [a,b,*], Antonia Bär [a], Suzanne Dorfman [a], Zlata Vukadinovic [a], Yoshiki Sawa [c], Axel Haverich [a,b], Andres Hilfiker [a]

[a] *Leibniz Research Laboratories for Biotechnology and Artificial Organs (LEBAO), Hannover Medical School, Hannover, Germany*
[b] *Department of Cardiac, Thoracic, Transplantation and Vascular Surgery, Hannover Medical School, Hannover, Germany*
[c] *Department of Cardiovascular Surgery, Osaka University Graduate School of Medicine, Suita, Japan*

Received 1 October 2009; received in revised form 30 January 2010; accepted 4 February 2010

Abstract

Objectives: A persistent problem in generating a functional myocardial patch is maintaining contractions in a thicker construct. Thus far, we have successfully created contracting constructs with a defined directionality by seeding neonatal rat cardiomyocytes (CMs) on decellularised porcine small-intestinal submucosa (SIS). Here, we report our efforts in generating a thicker contracting construct by combining CM cell sheets with CM-seeded SIS. **Methods:** Porcine SIS was decellularised, opened along the longitudinal axis, fixed in a metal frame (45 mm × 25 mm) and seeded onto the submucosal side with neonatal rat CMs at a density of 1.8×10^5 cells cm^{-2}. CM sheets were prepared using temperature-responsive dishes by seeding CMs at a density of 4.0×10^5 cells cm^{-2}. Three days after CM seeding, one- or three-layered CMs sheet(s) were stacked onto seeded SIS. Construct contraction was observed for an additional 10 days followed by histological analysis. **Results:** Stacked CM sheets contracted spontaneously and synchronously with seeded SIS after adherence. A large portion of analysed constructs showed a defined contraction direction, parallel to the longitudinal axis (seeded SIS: 83%, seeded SIS + 1 sheet: 70%, seeded SIS + 3 layered sheets: 71%). This finding was in agreement to the histological finding of aligned CMs parallel to the longitudinal axis. The thickness of seeded SIS with and without three-layered sheets was approximately 800 μm and 500 μm, respectively. **Conclusions:** By combining layered CM sheets with CM-seeded SIS, a three-dimensional myocardial patch with contraction in a defined direction was successfully generated. This may represent an intermediate step to a multiple layered, vascularised contractile myocardial graft.

Keywords: Tissue engineering; Small-intestinal submucosa; Cell sheet; Myocardial patch

1. Introduction

A major aim of tissue engineering is the production of a functional three-dimensional structure, aimed to restore, support or supersede native tissue function. Thus far, multiple tissue-engineered constructs have been developed and clinically applied since the term 'tissue engineering' was first introduced in 1987 [1]. Above all, engineering of myocardial tissue may become a pressing need in an ageing society with increasing cardiovascular morbidity [2]. Although several reports of producing cardiac tissue have been made since the late 1950s, engineering a fully functional and transplantable heart muscle has not yet been achieved due to the structural and functional complexity of native heart muscle [1–3].

Research conducted by Zimmermann and Zhao [3,4] has suggested three potential approaches to construct functional contractile cardiac tissue: (1) seeding cardiomyocytes (CMs) on a synthetic or biological scaffold; (2) using soluble collagen and other extracellular matrix (ECM) components to entrap CMs; and (3) stacking CM sheets to form multilayered cardiac muscle constructs. With respect to approach (1), our laboratory has successfully developed a contracting artificial myocardial tissue by seeding CM on a collagen scaffold [5]. Progress in this direction was achieved through the replacement of the collagen scaffold with decellularised porcine small-intestinal submucosa (SIS) as the matrix. When seeded with neonatal rat CM, a contracting construct with a defined direction was generated [6].

Cell sheet technology (approach 3) has several advantages; for example, the preservation of cell-to-cell connec-

☆ Presented at the 23rd Annual Meeting of the European Association for Cardio-thoracic Surgery, Vienna, Austria, October 18–21, 2009.

☆☆ *Sources of funding*: This study was supported by the CORTISS Foundation. H.H. received a fellowship from the Japan Heart Foundation and the Uehara Memorial Foundation.

* Corresponding author. Address: Leibniz Research Laboratories for Biotechnology and Artificial Organs (LEBAO), Hannover Medical School, Carl-Neuberg-Strasse 1, D-30625 Hannover, Germany. Tel.: +49 511 532 8913; fax: +49 511 532 8819.
E-mail address: Hata.Hiroki@mh-hannover.de (H. Hata).

1010-7940/$ – see front matter
doi:10.1016/j.ejcts.2010.02.009

Please cite this article in press as: Hata H, et al. Engineering a novel three-dimensional contractile myocardial patch with cell sheets and decellularised matrix. Eur J Cardiothorac Surg (2010), doi:10.1016/j.ejcts.2010.02.009

tion with ECM, the maintenance of electrophysiological and contractile performance, the feasibility of stacking multiple sheets and the independence from potentially immunogenic or pathogenic scaffold materials [1,7]. However, the maximum thickness and strength achievable, relative to native tissue, remains equivocal. Our laboratory has investigated the transfer of cell sheets of various origins, as a regenerative therapy option in different animal models [8,9] and in a clinical study in Osaka University.

Decellularised porcine SIS is an acellular ECM rich in collagen, glycosaminoglycans and growth factors, and been characterised as a complete absorbable biocompatible framework [10]. As a result of these characteristics, it has great potential for use in both *ex vivo* tissue engineering and in reconstructive surgery. SIS and similar ECM scaffolds, for example, decellularised porcine urinary bladder matrices have also been applied in animal models of cardiac repair [11,12].

Herein, we describe our next step towards an implantable myocardial patch combining our previous success with CM-seeded SIS and CM cell sheets.

2. Materials and methods

2.1. Animal care

This work was approved by the Institutional Review Board and the Institutional Animal Care and Use Committee protocols of Hannover Medical School. All animals received humane care in compliance with the European Convention on Animal Care.

2.2. Decellularisation of porcine SIS

Porcine small intestine was harvested from anaesthetised German Landrace pigs weighing 20–25 kg and cut into short segments. After mechanical removal of tunica mucosa and tunica serosa, segmented intestines were chemically decellularised using a modified method of Meezan et al. [13]. In brief, decellularisation was performed using 4% sodium-deoxycholate and 0.1% sodiumazide under continuous shaking at 4 °C for 2 h. SISs were washed with phosphate-buffered saline (PBS) containing 0.1% neomycin sulphate and 1% penicillin–streptomycin solution under continuous shaking for 7 days at 4 °C. Following the last wash, SISs were sterilised by 150 Gy gamma-ray irradiation for 75 min. Just before use, they were cut open along the longitudinal axis and fixed on a 45 mm × 25 mm metal frame.

2.3. Preparation of CM-seeded SIS and CM sheet

Neonatal rat CMs were isolated as described previously [14]. In brief, ventricles from 1- to 2-day-old Sprague Dawley rats were minced in ADS buffer (116 mM NaCl, 20 mM HEPES, 10 mM NaH_2PO_4, 5.4 mM KCl, 0.8 mM $MgSO_4$ and 5.6 mM glucose) and enzymatically digested with type II collagenase (Worthington, Lakewood, NJ, USA) and pancreatin (Sigma–Aldrich, St. Louis, MO, USA) at 37 °C. CMs were enriched in the primary CM isolates either by differential centrifugation through discontinuous Percoll gradient or with the preplating procedure. For preplating, CM isolates in culture medium were cultivated in flasks for 1 h. Following 1 h, the remaining supernatant in the flask contained an enriched CM fraction. Purification of CM by a discontinuous Percoll gradient was prepared as described before [15] using two density solutions, 1.062 and 1.082 g ml^{-1}, made from Percoll reagent (GE Healthcare). The collected cells after Percoll gradient centrifugation were seeded at a density of 1.8×10^5 cells cm^{-2} onto the submucosa side of SIS fixed in a metal frame. The SIS with cells were cultivated in 1:4 Dulbecco's Modified Eagle's Medium (Gibco, Invitrogen):medium 199 (PAA, Pasching, Austria), 10% foetal calf serum (PAA), 5% horse serum (Gibco) and 1% penicillin–streptomycin in a humidified 37 °C atmosphere with 5% CO_2.

For the generation of cell monolayer sheets, preplated CMs were cultivated in temperature-responsive dishes as described before [7]. In brief, CMs were seeded at a density of 4.0×10^6 cells per poly(N-isopropylacrylamide) grafted temperature-responsive dish (UpCell; Cellseed, Tokyo, Japan) with a diameter of 35 mm and incubated in culture medium for 3 days.

2.4. Transfer of CM sheet onto decellularised SIS

After 3 days of cultivation, CM cell sheets were detached through a temperature change from 37 °C to 20 °C for approximately 30 min. After detachment, one cell sheet ($n = 24$) or three-layered cell sheets ($n = 18$) were stacked onto a CM-seeded SIS according to previously described procedures [7]. Briefly, the entire CM sheet with media was gently aspirated and transferred onto the SIS. Media was then gently dropped onto the centre of the sheet to spread the folded parts. Excess media was aspirated to allow the cell sheet to adhere to the SIS. After 30 min and using the same protocol, additional CM sheets were transferred and spread onto the formerly attached cell sheet. Approximately 30 min were found to be sufficient for adhesion of the layered sheet(s). In addition, one CM sheet on an un-seeded SIS ($n = 13$) and CM-seeded SIS without CM sheet ($n = 12$) were prepared. All constructs were incubated at 37 °C for an additional 10 days and the culture medium was changed every 2 days.

2.5. Assessment of cell population

Cells after Percoll gradient or preplating were seeded on 10 temperature-responsive dishes (3.0×10^6 cells per dish), respectively, and incubated in a culture medium as described above for 1 day. After fixation with 4% formaldehyde, cells were stained with monoclonal anti-α-sarcomeric actinin (Sigma) or anti-prolyl-4β-hydroxylase (Acris, Hiddenhausen, Germany). Nuclei were counterstained with 4′,6-diamidino-2-phenylindole (DAPI) (Sigma). The images were photographed using an inverted research microscope (Axio Observer A1, Zeiss). Cell population percentages were calculated by dividing the number of respective cells by the total number of cells. Four randomly selected optical fields (0.083 mm^2) per dish were analysed and an image analysis software (ImageJ 1.40 g, Wayne Rasband, NIH, USA) was used.

Please cite this article in press as: Hata H, et al. Engineering a novel three-dimensional contractile myocardial patch with cell sheets and decellularised matrix. Eur J Cardiothorac Surg (2010), doi:10.1016/j.ejcts.2010.02.009

2.6. Microscopic and macroscopic observation

All constructs were observed by means of an inverted optical microscope (CKX41, Olympus) to count the synchronous contraction rate and to observe the contraction direction. The contractile direction, within approximately 30° from the longitudinal axis of the SIS, was defined as an oriented contraction parallel to the longitudinal axis. The ratio of constructs showing oriented contractions was calculated by dividing the number of respective myocardial grafts by the total number of myocardial grafts. Microscopic images of contracting CM sheets on SIS were recorded using a motorised inverted research microscope (Axio Observer Z1, Zeiss). Macroscopic images of contracting myocardial patches were also recorded using a digital movie camera (DMX-HD2, SANYO).

2.7. Histological analysis

For assessment of collagen fibre alignment, a small piece of decellularised SIS was fixed with 4% paraformaldehyde and stained with anti-collagen I (Sigma) detected by Alexa Fluor 488 (Molecular Probes, Eugene). For characterisation of the seeded cells and cell sheets on SIS, samples were cut into approximately 4 cm^2 squares, fixed with 4% paraformaldehyde and stained with Alexa Fluor 488-conjugated phalloidin (Molecular Probes) or monoclonal anti-α-sarcomeric actinin and Alexa Fluor 488 (Molecular Probes). Cell nuclei were counterstained with DAPI. Additional samples were fixed with 10% formalin, embedded in paraffin, cut into 6-μm cross-sections, and stained with haematoxylin and eosin or monoclonal anti-connexin 43 (Sigma) and Alexa Fluor 488. Connexin 43-stained samples were counterstained with DAPI. Stained sections were analysed and documented using an inverted research microscope (Axio Observer A1).

2.8. Statistics

All data are presented as mean ± standard deviation.

3. Results

3.1. Decellularised SIS

Decellularised SIS was pliable, durable and easily stretched onto a metal frame (Fig. 1(A) and (B)). Collagen fibres in the decellularised SIS were oriented along the longitudinal axis (Fig. 1(C)).

3.2. Cell population after Percoll gradient and preplating

CMs and fibroblasts were identified through staining for α-sarcomeric actinin and prolyl-4β-hydroxylase, respectively. The cell suspension after Percoll gradient centrifugation contained 86.9 ± 3.8% CM and 10.5 ± 1.0% fibroblasts, while preplating isolates contained 74.6 ± 3.6% CM and 21.6 ± 5.6% fibroblasts.

SIS were seeded with both CM isolates; however, SIS seeded with preplated CM isolates resulted in a less synchronous contraction pattern and over a shorter duration than SIS seeded with the Percoll CM isolates (data not shown). Similarly, CM cell sheets were made with both CM isolates. Cell sheets and subsequent stacking made with Percoll CM isolates resulted in a less tight adhesion as shown by cross-section histological assessment (Fig. 2). Based on these data, CM from Percoll isolates were used as the cell source for direct seeding onto the SIS, and CM cell sheets stacked on the SIS were made with preplated CM isolates.

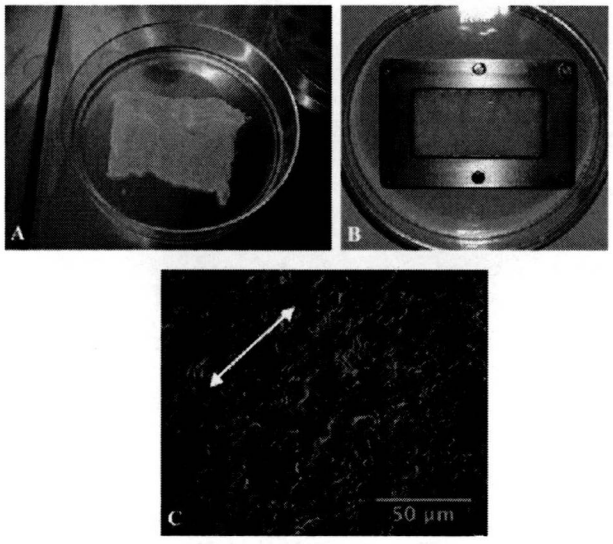

Fig. 1. Decellularised porcine small-intestinal submucosa (SIS) (A), fixed in a metal frame such that the long axis of the SIS was parallel to the long axis of the metal frame (B). Anti-collagen I staining revealed that collagen fibre in SIS aligned along the longitudinal axis (C). Scale bars: 50 μm.

3.3. Macroscopic and microscopic observation

All Percoll CM-seeded SIS started to contract spontaneously 1–2 days after initial CM seeding. After lowering culture temperature from 37 °C to 20 °C, CM cell sheets

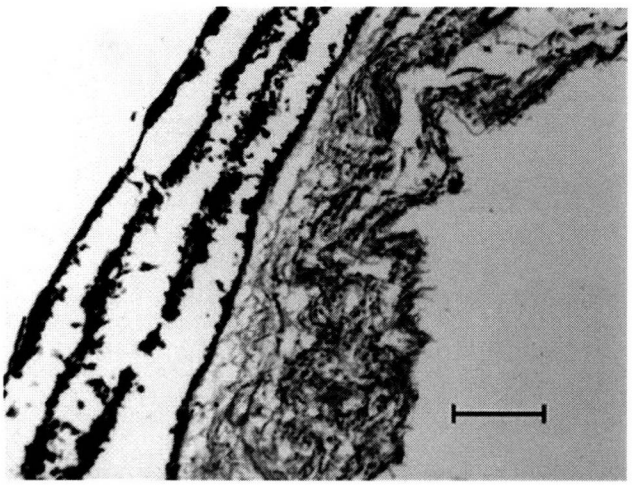

Fig. 2. Haematoxylin and eosin staining of a cross-sectional slice of a myocardial patch made with three-layered Percoll-enriched cardiomyocyte (CM) sheets on a CM-seeded small-intestinal submucosa (SIS). CM sheets did not adhere to one another or to the seeded SIS. Scale bars: 200 μm.

Please cite this article in press as: Hata H, et al. Engineering a novel three-dimensional contractile myocardial patch with cell sheets and decellularised matrix. Eur J Cardiothorac Surg (2010), doi:10.1016/j.ejcts.2010.02.009

Fig. 3. Macroscopic appearance of seeded SIS with three-layered cardiomyocyte sheets.

spontaneously detached as a single unit maintaining contractility without enzymatic treatment. Initially, a transferred CM sheet shrank to some extent, and had asynchronous contractions in multiple directions. As shown in Fig. 3, the cell sheet could be manipulated to lie flat on either seeded or un-seeded SIS. After stacking, the cell sheets placed on SIS collectively contracted in a defined direction parallel to the longitudinal axis of the SIS (Supplemental Video 1). The wave-like contraction pattern was observed for both CM sheets layered on CM-seeded SIS and un-seeded SIS. All constructs, regardless of the number of cell sheets, began contracting a few minutes after transfer. Approximately 50% of all myocardial patches with one or three cell sheet(s) on CM-seeded SIS contracted until day 10 after sheet transplantation, while un-seeded SIS with one CM sheet contracted for only 4 days after cell sheet transfer. A large proportion of analysed constructs showed an oriented contraction parallel to the longitudinal axis of the SIS 3 days after cell sheet transfer; CM-seeded SIS without cell sheets: 83%, CM-seeded SIS with one CM sheet: 70%, CM-seeded SIS with three-layered CM sheets: 71%. Macroscopic observation of CM-seeded SIS with three-layered CM sheets with a defined contraction orientation and parallel to the longitudinal axis of SIS is shown in Supplemental Video 2.

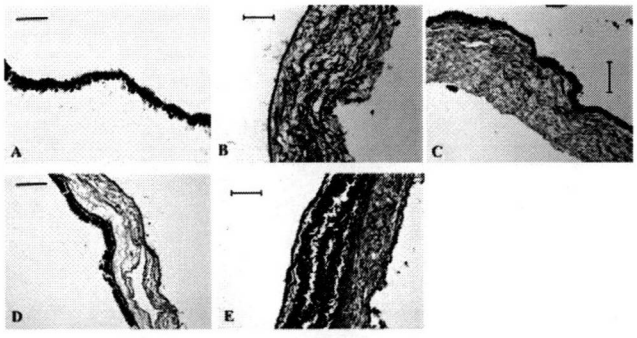

Fig. 4. Haematoxylin and eosin staining of cross-sectional slices of myocardial patches. Small-intestinal submucosa (SIS) was seeded with Percoll cardiomyocytes (CM), cell sheets were made with preplated CM. (A) single CM cell sheet; (B) decellularised porcine SIS; (C) CM-seeded SIS; (D) CM-seeded SIS with 1 CM sheet; (E) CM-seeded SIS with three-layered CM sheets. Scale bars: 100 μm (A), 200 μm (B–E).

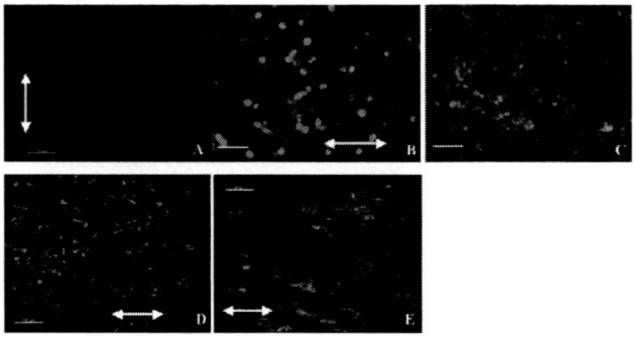

Fig. 5. Immunohistochemical assessment of decellularised small-intestinal submucosa (SIS) seeded with cardiomyocytes (CM) (A and B), CM sheet detached from the temperature-responsive dish (C), and CM sheet on seeded SIS (D and E). Cells were stained with phalloidin (A and C) or anti-α-sarcomeric actinin (B, D and E). Nuclei were stained with DAPI (A–E). Note orientation of CM cell sheet on seeded SIS (D and E) and seeded CM on SIS (A and B), which are consistent with the longitudinal axis of SIS indicated by white arrows. Scale bars: 50 μm (A, C and E), 100 μm (B and D).

3.4. Histological analysis

Cross-sectional slices stained with haematoxylin and eosin are shown in Fig. 4. As shown in Fig. 4(A) and (B) respectively, one CM cell sheet has a thickness of approximately 40–50 μm and a decellularised SIS is approximately 300–500 μm thick. No remnant cells were detected in the decellularised SIS. Seeded Percoll CM attached to the decellularised SIS (Fig. 4(C)). Layered CM cell sheets adhered to each other or to the CM-seeded SIS (Fig. 4(D) and (E)), and a seeded SIS layered with three CM sheets measured approximately 600–800 μm thick.

Immunohistochemical analysis with phalloidin and anti-α-sarcomeric actinin confirmed that the seeded Percoll CM aligned parallel to the longitudinal axis of the SIS (Fig. 5(A) and (B)). Although CM in the detached cell sheet appeared disordered and without alignment (Fig. 5(C)), once attached to the seeded SIS, the CM within the cell sheet aligned in a similar direction to the Percoll CM (along the longitudinal axis of the SIS) (Fig. 5(D) and (E)). These findings support the macroscopic and microscopic observations reported above.

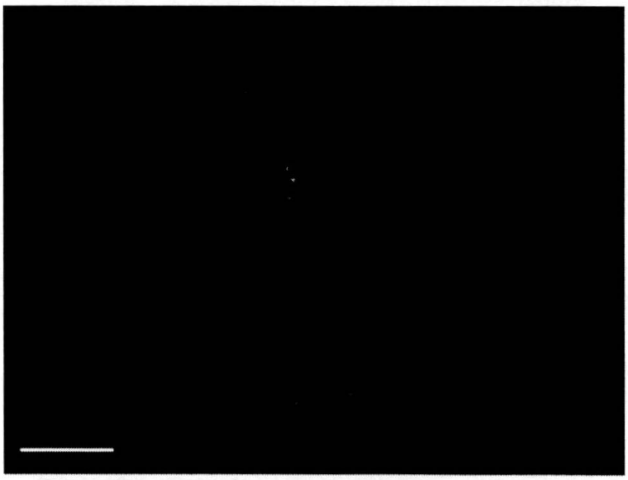

Fig. 6. Anti-connexin 43 staining revealed gap-junctions throughout three-layered cardiomyocyte sheets on seeded small-intestinal submucosa (SIS). Nuclei were counterstained with DAPI. Scale bars: 100 μm.

Please cite this article in press as: Hata H, et al. Engineering a novel three-dimensional contractile myocardial patch with cell sheets and decellularised matrix. Eur J Cardiothorac Surg (2010), doi:10.1016/j.ejcts.2010.02.009

Anti-α-sarcomeric actinin staining also revealed the typical striated pattern of the CM in both the Percoll-seeded cells on SIS and in the CMs of the attached sheets (Fig. 5(B), (D) and (E)). Immunohistochemical staining with anti-connexin 43 demonstrated a diffuse expression of connexin 43 within the three-layered CM sheets on the seeded SIS (Fig. 6).

4. Discussion

Cell-transplantation therapy, to treat damaged myocardium, has been widely studied and has resulted in positive, albeit limited, effects in clinical trials [16]. Despite early success, problems still remain including method of cell delivery, poor graft survival, functional integration and post-transplantation arrhythmias [17]. Moreover, changes in the ECM, which are regarded to play a pivotal role for cell survival, differentiation, proliferation, metabolism and integrative function, are not taken into consideration with this intervention [18]. The emergence of a second regenerative therapy using a combination of cells and ECM provide greater advantages towards the engineering of a three-dimensional functional myocardial patch [18,19]. To this point, the present study demonstrated the feasibility of generating a contractile myocardial patch by combining a decellularised biological matrix (SIS) with CM cell sheets. Moreover, we show that CM sheets can be layered on SIS without disrupting contractile alignment and function of the CM. Thus, our results represent an important intermediate step towards the engineering of a complex, multilayered contractile myocardial patch.

Decellularised SIS is an ideal matrix for tissue engineering and remodelling due in part, to its intact ECM. The ECM of SIS consists primarily of collagens (types I, III and VI), and also glycosaminoglycans, for example, hyaluronic acid, chondroitin sulphate A and B, heparin, and heparan sulphate, and glycoproteins, for example, fibronectin. In addition, several cytokines are produced, including basic fibroblast growth factor and transforming growth factor-β, which together induce cellular migration, proliferation and differentiation, early capillary ingrowth and ultimately, endothelialisation. In addition, decellularised SIS has been previously characterised as a complete absorbable biocompatible framework with a high resistance towards infection [20,21]. Moreover, inherent SIS fibre alignment is along the longitudinal axis of the small intestine [22,23], which enables us to induce a 'preferred' cellular alignment without mechanical stimulation. Typically, the native cell alignment in an artificial tissue-engineered system is accomplished either by mechanical stimulation or by using a patterned scaffold requiring complex devices or materials [1,4]. When SIS is used; however, it leads to an orthotropic mechanical behaviour of the scaffold, with the preferred fibre direction showing great stiffness and strength [22,23].

Cell sheet engineering is a well-established technique using cells from various sources, and has already been investigated in a clinical setting [24]. CM cell sheets are unique due to their contractile ability. The most distinct advantage of CM cell sheet engineering is that they can be easily layered while maintaining electrically communicative pulsation supported through gap-junctions [7,8]. To this point, anti-connexin 43 immunohistochemistry revealed diffuse gap-junctions within the three-layered CM sheets on the CM-seeded SIS. This abundant detection of connexin 43 suggested the formation of an electrical syncytium throughout the cell sheets and connection with CM seeded on SIS. This finding, in addition to the intact ECM of the SIS, provides strong support for the coupling of these two technologies.

Despite initial success, additional questions with respect to the detailed character of a tissue-engineered heart patch remain unanswered. First, the strength and durability of the contractile forces generated by the layered CM sheets are unknown. These assessments are crucial as the patch is being generated to replace scar tissue in the left ventricle of the heart. A previous study has shown that SIS itself or a similar ECM, for example, porcine urinary bladder matrix, could substitute for the right ventricular wall [11] or even the left ventricular wall [12] in a large animal model. However, in that study, the patches were implanted as four ECM-layered patches based on the idea that the mechanical behaviour of a single layer of SIS is insufficient for most load-bearing applications [22]. Recently, our colleagues reported a successful implantation of an autologous vascularised matrix from a porcine small bowel segment without mucosa to the right ventricular wall of the pig [25]. While it differs from our myocardial construct in its characteristics, its thickness is comparable. The results from this study suggest that one SIS layer may, in fact, be sufficient.

A second question is whether the ECM provided by the SIS is similar or adaptable to a native-like ECM, to support the contractility of the ventricle [25]. While the CM cell sheet has an ECM of ventricular origin, the effect of the intestinal ECM on myocardial function has not been determined. Cell source is the subject of the third question. For clinical application, the use of autologous, allogenic or xenogenic CMs may be problematic. Of course, this matter is universal in cardiac tissue engineering and most cell-based therapies. To this point, embryonic and adult stem cells, or induced pluripotent stem cell-based approaches will play a central role in the near future [1].

Finally, the engineering of myocardial heart patch with CM cell sheets is limited by the thickness generated through sheet stacking. In this study, a myocardial patch with a thickness of roughly 800 μm was built. Although possible, more cell sheets can be continuously layered; however, supplying sufficient oxygen and nutrients will challenge the viability of a thicker construct. Although these issues will be addressed to determine the future clinical application, the present preliminary study shows the novel development of a pulsatile, thicker myocardial patch with unidirectional contractions and proposes a new strategy for regenerative therapy for cardiac dysfunction.

In conclusion, by combining a CM-seeded matrix with CM sheets, a multilayered and contracting myocardial graft was successfully generated. Moreover, our novel myocardial patch is a good foundation for our ultimate goal; a vascularised three-dimensional myocardial graft.

References

[1] Eschenhagen T, Zimmermann WH. Engineering myocardial tissue. Circ Res 2005;97:1220–31.

Please cite this article in press as: Hata H, et al. Engineering a novel three-dimensional contractile myocardial patch with cell sheets and decellularised matrix. Eur J Cardiothorac Surg (2010), doi:10.1016/j.ejcts.2010.02.009

[2] Haverich A. Cardiac tissue engineering. Eur J Cardiothorac Surg 2008;34:227–8.
[3] Zimmermann WH, Didie M, Döker S, Melnzchenko I, Naito H, Rogge C, Tiburcz M, Eschenhagen T. Heart muscle engineering: an update on cardiac muscle replacement therapy. Cardiovasc Res 2006;71:419–29.
[4] Zhao YS, Wang CY, Li DX, Zhang XZ, Qiao Y, Guo XM, Wang XL, Dun CM, Dong LZ, Song Y. Construction of a unidirectionally beating 3-dimensional cardiac muscle construct. J Heart Lung Transplant 2005;24:1091–7.
[5] Kofidis T, Akhyari P, Boublik J, Theodorou P, Martin U, Ruhparwar A, Fischer S, Eschenhagen T, Kubis HP, Kraft T, Leyh R, Haverich A. In vitro engineering of heart muscle: artificial myocardial tissue. J Thorac Cardiovasc Surg 2002;124:63–9.
[6] Bär A, Haverich A, Hilfiker A. Cardiac tissue engineering: "reconstructing the motor of life". Scand J Surg 2007;96:154–8.
[7] Shimizu T, Yamato M, Isoi Y, Akutsu T, Setomaru T, Abe K, Kikuchi A, Umezu M, Okano T. Fabrication of pulsatile cardiac tissue grafts using a novel 3-dimensional cell sheet manipulation technique and temperature-responsive cell culture surfaces. Circ Res 2002;90:e40.
[8] Miyagawa S, Sawa Y, Sakakida S, Taketani S, Kondoh H, Memon IA, Imanishi Y, Shimizu T, Okano T, Matsuda H. Tissue cardiomyoplasty using bioengineered contractile cardiomyocyte sheets to repair damaged myocardium: their integration with recipient myocardium. Transplantation 2005;80:1586–95.
[9] Hata H, Matsumiya G, Miyagawa S, Kondoh H, Kawaguchi N, Matsuura N, Shimizu T, Okano T, Matsuda H, Sawa Y. Grafted skeletal myoblast sheets attenuate myocardial remodeling in pacing-induced canine heart failure model. J Thorac Cardiovasc Surg 2006;32:918–24.
[10] Hodde J. Naturally occurring scaffolds for soft tissue repair and regeneration. Tissue Eng 2002;8:295–308.
[11] Badylak S, Obermiller J, Geddes L, Matheny R. Extracellular matrix for myocardial repair. Heart Surg Forum 2003;6:E20–26.
[12] Robinson KA, Li J, Mathison M, Redkar A, Cui J, Chronos NA, Matheny RG, Badylak SF. Extracellular matrix scaffold for cardiac repair. Circulation 2005;112:I135–143.
[13] Meezan E, Hjelle JT, Brendel K. A simple versatile; nondisruptive method for the isolation of morphologically and chemically pure basement membranes from several tissues. Life Sci 1975;17:1721–32.
[14] Wollert KC, Taga T, Saito M, Narazaki M, Kishimoto T, Glembotski CC, Vernallis AB, Heath JK, Pennica D, Wood WI, Chien KR. Cardiotrophin-1 activates a distinct form of cardiac muscle cell hypertrophy. Assembly of sarcomeric units in series VIA gp130/leukemia inhibitory factor receptor-dependent pathways. J Biol Chem 1996;271:9535–45.
[15] Iwaki K, Sukhatme VP, Shubeita HE, Chien KR. Alpha- and beta-adrenergic stimulation induces distinct patterns of immediate early gene expression in neonatal rat myocardial cells. fos/jun expression is associated with sarcomere assembly; Egr-1 induction is primarily an alpha 1-mediated response. J Biol Chem 1990;265:13809–17.
[16] Hagège AA, Marolleau JP, Vilquin JT, Alhéritière A, Peyrard S, Duboc D, Abergel E, Messas E, Mousseaux E, Schwartz K, Desnos M, Menasché P. Skeletal myoblast transplantation in ischemic heart failure: long-term follow-up of the first phase I cohort of patients. Circulation 2006;114(1 Suppl.):I108–13.
[17] Menasché P, Alfieri O, Janssens S, McKenna W, Reichenspurner H, Trinquart L, Vilquin JT, Marolleau JP, Seymour B, Larghero J, Lake S, Chatellier G, Solomon S, Desnos M, Hagège AA. Circulation 2008;117:1189–200.
[18] Akhyari P, Kamiya H, Haverich A, Karck M, Lichtenberg A. Myocardial tissue engineering: the extracellular matrix. Eur J Cardiothorac Surg 2008;34:229–41.
[19] Chachques JC, Trainini JC, Lago N, Cortes-Morichetti M, Schussler O, Carpentier A. Myocardial Assistance by Grafting a New Bioartificial Upgraded Myocardium (MAGNUM trial): clinical feasibility study. Ann Thorac Surg 2008;85:901–8.
[20] Lindberg K, Badylak SF. Porcine small intestinal submucosa (SIS): a bioscaffold supporting in vitro primary human epidermal cell differentiation and synthesis of basement membrane proteins. Burns 2001;27:254–66.
[21] Mertsching H, Walles T, Hofmann M, Schanz J, Knapp WH. Engineering of a vascularized scaffold for artificial tissue and organ generation. Biomaterials 2005;26:6610–7.
[22] Badylak SF. The extracellular matrix as a biologic scaffold material. Biomaterials 2007;28:3587–93.
[23] Sacks MS, Gloeckner DC. Quantification of the fiber architecture and biaxial mechanical behavior of porcine intestinal submucosa. J Biomed Mater Res 1999;46:1–10.
[24] Yang J, Yamato M, Shimizu T, Sekine H, Ohashi K, Kanzaki M, Ohki T, Nishida K, Okano T. Reconstruction of functional tissues with cell sheet engineering. Biomaterials 2007;28:5033–43.
[25] Tudorache I, Kostin S, Meyer T, Teebken O, Bara C, Hilfiker A, Haverich A, Cebotari S. Viable vascularized autologous patch for transmural myocardial reconstruction. Eur J Cardiothorac Surg 2009;36:306–11.

Appendix A. Conference discussion

Dr P. Menasche *(Paris, France)*: Thank you and your colleagues for providing additional evidence that the expected benefits of cell therapy are likely to be enhanced by some form of cell scaffolding. That said, I have two questions.

The first is that if one looks at the improvement in the contraction patterns in your composite biomaterial, the composite – I mean the SIS plus the cell sheets, it turns out that it might simply reflect the fact that you had many more cells in your combined biomaterial compared with either treatment alone. You had five times more cells in the combined scaffold. So keeping in mind that the widespread clinical application of any technique requires it to be as simple as possible, my naive question is: Would it be conceivable that you would get a similar result if you simply increased the cell-seeding density on your SIS to match the final number of cells that you have got when you have combined the two materials? And that would probably be true also for explaining the increased thickness. Again you had such a disparity in the numbers of cells between the groups that it might be one explanation for your results. So is there any rationale for combining the two scaffolds? And you probably should tell us what is the contribution of a given material to the other instead of using just a single material with more cells, contractile cells, on board.

My second question is that you have shown us that there was some expression of connexin 43. Did you do some dye experiments documenting that you have an effective transmission of the impulses from one cell to the other? And more importantly, we realize that this is an in vitro study, but do you have any in vivo data allowing you to speculate on how these epicardially-delivered cells would couple with the underlying host cardiomyocytes, because obviously this is critical.

Dr Hata: As to your first question, we seeded about 180,000 cells/sq cm onto SIS and 400,000 cells/cm sq/cardiomyocyte sheet. So, as you mentioned, these cell numbers do not match. I think we need more cells to generate cell sheet than to seed on SIS. We seeded cardiomyocyte on SIS for the sake of the affinity for cardiomyocyte sheets, and we tested also cardiomyocyte sheet on un-seeded SIS but that construct did not contract longer than 4 days in a defined direction.

And the reason we used SIS as a scaffold is not only to gain thickness, but also looking toward the next step in our research utilizing vascularised SIS, so-called BioVaM. We would like to use such vascularised SIS as our next step, so we tested the feasibility of SIS in combination with cell sheets.

And as for the second question, in fact we didn't do any functional testing or *in vivo* studies. I think it may be the focus of our future studies. However, when we think about the animal model, we used here neonatal rat cardiomyocytes. So when we use a large animal model, we must think about a suitable cell source, such as iPS cells.

And you mentioned connexin 43 – I'm sorry what was your question?

Dr Menasche: The question is: Do you have any data, or can you speculate, on how cells which are delivered on the epicardium, which would be delivered on the epicardium, how you think they could couple with the cardiomyocytes of the recipient heart which are underneath?

Dr Vaage *(Oslo, Norway)*: Does Axel Haverich want to comment on this?

Dr Haverich: We did implant, also in large animal preparations, the SIS only, and we have seen coupling there. We only did these experiments to increase the thickness. Because we can do right atrial, right ventricular replacement at this point, but for left ventricular replacement we need to increase the thickness and this is why we have this combined approach. We have done electrophysiology and put a pacemaker lead on one side of the graft *in vitro* and have seen propagation of the impulse. With regard to your connexin question, we have seen propagation of the contraction towards the other end of the graft. So there is electrophysiological contact between the cells.

Appendix B. Supplementary data

Supplementary data associated with this article can be found, in the online version, at doi:10.1016/j.ejcts.2010.02.009.

Please cite this article in press as: Hata H, et al. Engineering a novel three-dimensional contractile myocardial patch with cell sheets and decellularised matrix. Eur J Cardiothorac Surg (2010), doi:10.1016/j.ejcts.2010.02.009

Clin Orthop Relat Res (2009) 467:3149–3155
DOI 10.1007/s11999-009-0899-2

SYMPOSIUM: TRIBUTE TO DR. MARSHALL URIST: MUSCULOSKELETAL GROWTH FACTORS

Synthetic Alginate is a Carrier of OP-1 for Bone Induction

Katsuhiko Nanno MD, Kenjiro Sugiyasu MD, Takashi Daimon PhD, Hideki Yoshikawa MD, PhD, Akira Myoui MD, PhD

Published online: 28 May 2009

Abstract Bone morphogenetic proteins (BMPs) can induce bone formation in vivo when combined with appropriate carriers. Several materials, including animal collagens and synthetic polymers, have been evaluated as carriers for BMPs. We examined alginate, an approved biomaterial for human use, as a carrier for BMP-7. In a mouse model of ectopic bone formation, the following four carriers for recombinant human OP-1 (BMP-7) were tested: alginate crosslinked by divalent cations (DC alginate), alginate crosslinked by covalent bonds (CB alginate), Type I atelocollagen, and poly-D,L-lactic acid-polyethyleneglycol block copolymer (PLA-PEG). Discs of carrier materials (5-mm diameter) containing OP-1 (3–30 μg) were implanted beneath the fascia of the back muscles in six mice per group. These discs were recovered 3 weeks after implantation and subjected to radiographic and histologic studies. Ectopic bone formation occurred in a dose-dependent manner after the implantation of DC alginate, atelocollagen, and PLA-PEG, but occurred only at the highest dose implanted with CB alginate. Bone formation with DC alginate/OP-1 composites was equivalent to that with atelocollagen/OP-1 composites. Our data suggest DC alginate, a material free of animal products that is already approved by the FDA and other authorities, is a safe and potent carrier for OP-1. This carrier may also be applicable to various other situations in the orthopaedic field.

One or more of the authors have received funding from Stryker Biotech K. K. (Tokyo, Japan) (AM) and from the Japan Science and Technology Agency (AM).
Each author certifies that his or her institution has approved the animal protocol for this investigation and that all investigations were conducted in conformity with ethical principles of research.
This work was performed at Department of Orthopaedic Surgery, Osaka University Graduate School of Medicine, Osaka, Japan.

K. Nanno, K. Sugiyasu, H. Yoshikawa (✉), A. Myoui
Department of Orthopaedic Surgery, Osaka University Graduate School of Medicine, 2-2 Yamadaoka, Suita, Osaka 565-0871, Japan
e-mail: yhideki@ort.med.osaka-u.ac.jp

T. Daimon, A. Myoui
Medical Center for Translational Research, Osaka University Hospital, 2-15 Yamadaoka, Suita, Osaka, Japan

Introduction

The repair capacity of human bone appears to depend on different very complex processes, such as vascularization, biomechanics, and topography. When damage is severe, as occurs with comminuted fractures or large bone defects after tumor resection, it is difficult for bone union to be achieved [6]. In such cases, autologous or allogenic bone grafting has been used. Autologous bone grafting is common and is still the gold standard, but has several disadvantages, including a limited supply of suitable bone and the risk of chronic pain, nerve damage, fracture, and cosmetic problems at the donor site. Allografts have no donor site problems, but there is the potential risk of disease or an immunologic reaction [10, 21]. For these reasons, the use of bone substitutes such as calcium phosphate-based porous ceramics has been increasing [18, 33]. These bioceramics are highly biocompatible and demonstrate osteoconduction, which is the ability to bind to bone matrix directly. However, they have no osteoinduction, which is the ability to induce new bone formation at ectopic sites.

Bone morphogenetic proteins (BMPs) belong to the transforming growth factor superfamily, are known to elicit new bone formation in vivo, and may play a leading role in

bone tissue engineering [36, 38]. To date, three types of BMP-based bone tissue engineering have been tried, which are cell therapy, gene therapy, and cytokine therapy [27]. Cell therapy involves the transplantation of autologous bone marrow mesenchymal cells after differentiation has been induced by BMP, but considerable resources and time are needed to culture the necessary cells [22, 34]. Gene therapy involves the transduction of genes encoding BMPs into cells at the site of damage [2, 7]. BMP-transduced cells may work more efficiently, compared with a single dose of recombinant cytokine therapy. However, gene therapy still has unsolved problems such as tumorigenesis and immunogenicity. Cytokine therapy involves the implantation of BMPs together with a carrier material that acts as a drug delivery system. We believe cytokine therapy is the most promising of these three approaches in terms of practical application. Cytokine therapy seems most convenient and safe, but the cost is very high because a large amount of BMP is required to achieve bone growth in humans. To increase the cost effectiveness of BMP, an appropriate carrier material is necessary.

Previous studies have indicated adequate in vivo new bone formation cannot be obtained by simply injecting a solution of BMP into the area where bone is needed [32]. For cytokine therapy, an appropriate carrier material is needed that retains BMP and releases it slowly, while serving as a scaffold for new bone formation [28, 29]. Several materials have already been evaluated as BMP carriers, including collagen obtained from animal sources [3, 11, 13, 31], synthetic polymers [14, 15, 19], tricalcium phosphate [17], and other inorganic materials [16]. Atelocollagen is a well-established BMP carrier, and has already been used clinically. PLA-PEG [20], one of the synthetic polymers, has been reported as a potent carrier for BMPs [23, 25, 26]. Although all of these materials can induce bone formation at ectopic and orthotopic sites, none of them has achieved widespread use because of disadvantages, such as the potential risk of disease transmission, fragility, stickiness, and difficulty in obtaining approval for clinical use [1, 4, 5, 14]. We therefore focused on alginate, which is already approved by the FDA for human use as a wound dressing and food additive [8, 37].

Alginate is a water-soluble linear polysaccharide extracted from brown seaweed that is composed of one to four linked α-L-gluronic and β-D-mannuronic acid monomers [9]. Gelation of alginate occurs as a result of crosslinking by divalent cations or covalent bonds [30]. Therefore, two types of alginate wound dressing products are available on the market and both effectively promote wound healing by maintaining a moist environment. One is an alginate crosslinked by divalent cations (DC alginate) and the other is an alginate crosslinked by covalent bonds (CB alginate).

To determine whether alginate can be a carrier for BMP, we compared four materials as carriers for OP-1(BMP-7) using the bone mineral content (BMC) measurement and alkaline phosphatase (ALP) activity measurement of the bone nodules ectopically induced by carrier materials/OP-1 composites. The four materials were DC alginate, CB alginate, atelocollagen, and PLA-PEG. We hypothesized: (1) BMC of bone nodules ectopically induced by DC alginate/OP-1 composite and/or CB alginate/OP-1 composite are equivalent or superior to those by atelocollagen and PLA-PEG; (2) ALP activity of bone nodules ectopically induced by DC alginate/OP-1 composite and/or CB alginate/OP-1 composite are equivalent or superior to those by atelocollagen and PLA-PEG by radiographic appearance and histology of the ectopic bone nodules; and (3) DC alginate and/or CB alginate have appropriate in vitro release kinetics of OP-1 equivalent to atelocollagen and PLA-PEG.

Materials and Methods

To verify our first hypothesis, we designed the following experiment (Experiment 1; Table 1). For each dose of OP-1 (3, 10, and 30 μg), 24 4-week-old male ICR mice were assigned to four equally sized independent groups after they were housed and acclimatized in cages with free access to food and water for 1 week. The four independent groups were DC alginate group, CB alginate group, atelocollagen group, and PLA-PEG group. The mice were anesthetized by intraperitoneal injection of pentobarbital. As reported previously [14, 15], carrier material/OP-1 composites were implanted beneath the fascia of the back muscles on the left side (one composite per animal). The experiment was designed under the assumption that the justifiable difference (effect size) between the atelocollagen group as a control and the other groups was 6 mg in BMC and the standard deviation within each group was 3 from the result of the previous study [24]. For the experiment to detect the difference at the 5% significance level with 90% power in the one-way analysis of variance, the necessary number of mice per group was six. Three weeks after implantation, these mice were killed and ectopic bone induced at the implantation site was harvested for further evaluation, including BMC measurement, radiography, and histological examination. The experimental protocol was approved by the Animal Experiment Committee of Osaka University, and the experiments were carried out in accordance with the Osaka University guidelines for care and use of laboratory animals.

To verify the second hypothesis, we repeated the Experiment 1 and obtained radiographs and measured ALP activity (Experiment 2; Table 1).

Table 1. Study groups and experimental design

Experiments	Carrier materials	Dose of OP-1	n	Examination
Experiment 1	DC alginate	3, 10, and 30 μg	18*	BMC, radiography, histology
	CB alginate	3, 10, and 30 μg	18*	BMC, radiography, histology
	Atelocollagen	3, 10, and 30 μg	18*	BMC, radiography, histology
	PLA-PEG	3, 10, and 30 μg	18*	BMC, radiography, histology
Experiment 2	DC alginate	3, 10, and 30 μg	18*	Radiography, ALP activity
	CB alginate	3, 10, and 30 μg	18*	Radiography, ALP activity
	Atelocollagen	3, 10, and 30 μg	18*	Radiography, ALP activity
	PLA-PEG	3, 10, and 30 μg	18*	Radiography, ALP activity

*: n = 6, each dose.

The BMC of the harvested discs was determined by dual-energy xray absorptiometry (DXA) using an animal bone densitometer (PIXImus; Lunar Corp, Madison, WI) and was expressed as milligrams per ossicle. Radiographs were obtained with a soft xray apparatus (MX-20 Faxitron®; Torrex and Micro Focus Systems, Wheeling, IL).

To measure ALP activity, the harvested discs were crushed, homogenized in 0.2% Nonidet® P-40 containing 1 mmol/L $MgCl_2$, and centrifuged at 10,000 rpm for 1 minute at 4°C. The supernatants thus obtained were assayed for ALP activity with an Alkaline Phospha B-Test Wako kit (Wako Pure Chemical Industries, Ltd, Osaka, Japan) using p-nitrophenyl phosphate (p-NP) as a substrate. The protein content was measured with a Pierce® BCA protein assay kit (Thermo Fisher Scientific Inc, Rockford, IL), and ALP activity was standardized by the protein content and expressed as nmol p-NP/minute/mg protein.

After radiography and BMC measurement, the samples were fixed in 10% neutral formalin, decalcified with ethylenediaminetetraacetic acid (pH 7.4), dehydrated in a graded ethanol series, and embedded in paraffin. One section per group with the largest tissue area (5-μm thick) were cut and stained with hematoxylin and eosin for observation under a light microscope. The formation of new bone, new bone marrow, degradation of the materials, and inflammatory change were evaluated by a pathologist (AM) and an orthopaedic surgeon (KN).

To verify the third hypothesis that DC alginate and/or CB alginate have appropriate in vitro release kinetics of OP-1, we incubated carrier materials/OP-1 composites in centrifuge tubes containing 1000 μL phosphate-buffered saline (PBS; Invitrogen, Carlsbad, CA) and kept for 21 days at 37°C. For each composite group, three samples were examined. The PBS in the tubes was replaced every 2 days, and then 100 μL was collected for assay after 24 hours. The amount of OP-1 was determined by measurement with a commercial BMP-7 ELISA kit (R&D Systems Inc, Minneapolis, MN) on days 1, 3, 7, 13, and 21 according to the manufacturer's instruction.

OP-1 (BMP-7 in a lyophilized 5% lactose formulation) was provided by Stryker Biotech (Hopkinton, MA). OP-1 was dissolved in distilled water at a concentration of 2 μg/μL. DC alginate (ARGODERM®; crosslinked by Ca^{2+}), CB alginate (KURABIO®), and atelocollagen (INSTAT®) were purchased from Smith & Nephew (London, UK), Koyo Sangyo Co, Ltd (Tokyo, Japan), and Johnson & Johnson (New Brunswick, NJ), respectively. PLA-PEG with a total molecular weight of 11,400 Da and a PLA:PEG molar ratio of 51:49 was synthesized and provided by Taki Chemicals Co, Ltd (Hyogo, Japan).

To prepare carrier material/OP-1 composites, sheets of DC alginate, CB alginate, and atelocollagen were cut into discs (5-mm diameter). Then 25 μL of a solution containing 3, 10, or 30 μg OP-1 was added dropwise to each disc, after which the discs were freeze-dried and stored at −20°C until implantation into mice. All procedures were carried out under sterile conditions.

PLA-PEG/OP-1 composites were prepared as described previously [25]. Briefly, 10 mg of the polymer was liquefied in 50 μL acetone and mixed with 3, 10, or 30 μg OP-1. Each mixture was evaporated to dryness to remove acetone in a safety cabinet, fabricated into a disc-shaped implant, and stored at −20°C until implantation into mice.

To verify the first and second hypotheses, we used one-way analysis of variance (ANOVA), followed by a post hoc Scheffe's test. For each of these statistical analyses, the data sets met the assumptions of normality ($p > 0.15$ by the Jarque-Bera test [12]) justifying the use of parametric models. All analyses were performed using the R software program (Version 2.8.1;R Foundation for Statistical Computing).

Results

With 3 μg OP-1, BMC of the new bone in the DC alginate group was greater than that in atelocollagen group ($p = 0.0234$) and PLA-PEG group ($p = 0.0009$). With

30 μg OP-1, however, we observed no differences among the DC alginate, atelocollagen, and PLA-PEG. On the other hand, BMC of CB alginate group was very low compared with the other groups (Fig. 1). The results suggest that the BMC of DC alginate group was superior to those of atelocollagen and PLA-PEG groups, especially with a low dose of OP-1.

In the DC alginate group, ALP activity was high independent of the OP-1 dose. With 3 μg OP-1, DC alginate/OP-1 composites exhibited higher ALP activity than atelocollagen group ($p = 0.0071$) and PLA-PEG group ($p = 0.0001$) (by Scheffe's test). ALP activity of the CB alginate group was very low compared with the other groups (Fig. 2). The results suggest that ALP activity of the DC alginate group was superior to those of atelocollagen and PLA-PEG groups, especially with a low dose of OP-1.

In the release study of OP-1, the maximum concentration of OP-1 in the supernatant was detected on Day 1, followed by a steady decline. The decline of OP-1 levels in the atelocollagen group was faster than that in the other groups. In the DC alginate group, the decrease of OP-1 levels was the slowest and the concentration of OP-1 was still higher than 200 ng/mL on Day 21 (Fig. 3). These data suggested that DC alginate retains OP-1 and releases it most slowly compared to atelocollagen and PLA-PEG.

In the additionally performed radiographic examination of the bone nodules, obvious bone formation was only detected in the DC alginate and atelocollagen groups with 3 μg OP-1 (Fig. 4A–D). In the CB alginate group, new bone formation was observed only with 30 μg OP-1. The results of the additionally performed histological examination were consistent with the radiographic findings. In the DC alginate and atelocollagen groups, abundant new bone formation that contained normal hematopoietic bone marrow was observed even at low dose of OP-1. In the CB alginate group, however, new bone formation was very poor at low dose of OP-1. With 30 μg OP-1, irrespective of the carrier materials, newly formed bone had a thin cortex

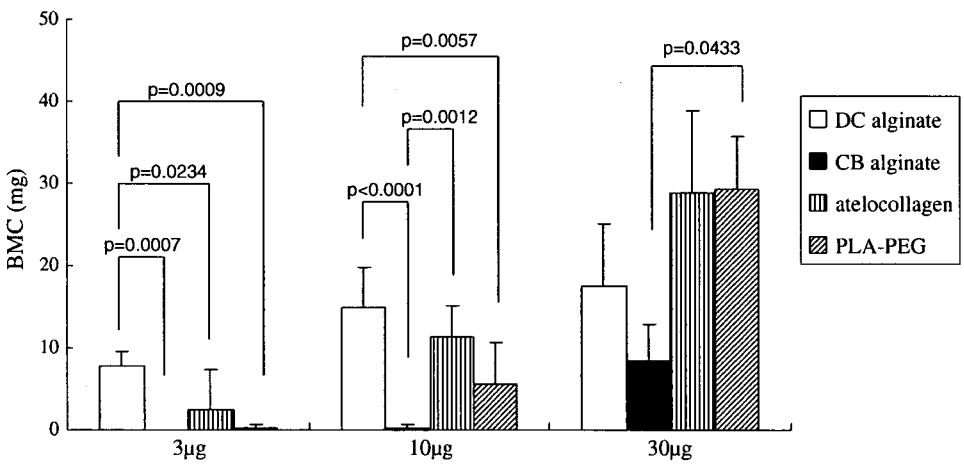

Fig. 1 In each carrier material group, BMC was measured by DXA using a PIXImus animal densitometer. BMC increased in an OP-1-dose dependent manner with every carrier material. With 3 μg and 10 μg OP-1, the BMC of the new bone in the DC alginate group was greater than that in the other groups.

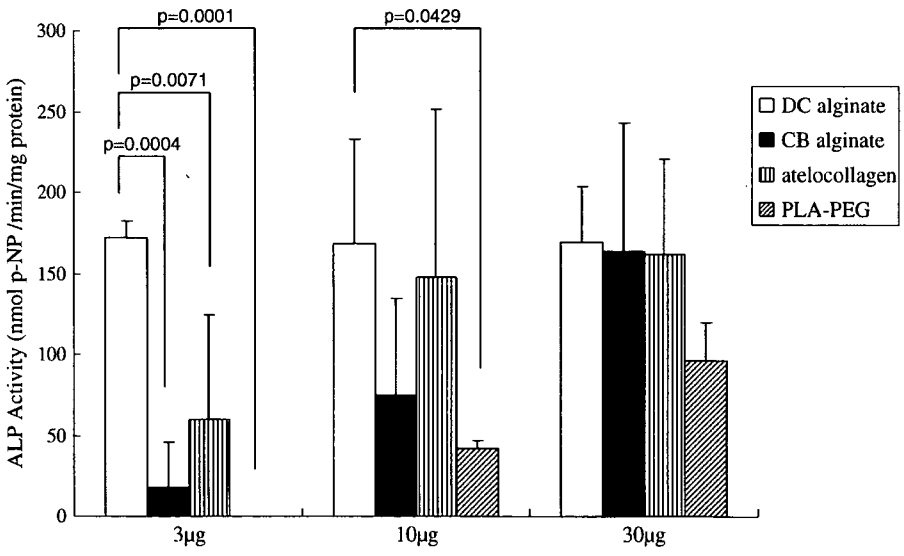

Fig. 2 ALP activity of ectopic bone was measured by using p-NP as a substrate. In the CB alginate, atelocollagen, and PLA-PEG groups, ALP activity increased in a dose-dependent manner. In the DC alginate group, ALP activity was relatively high independent of the dose of OP-1.

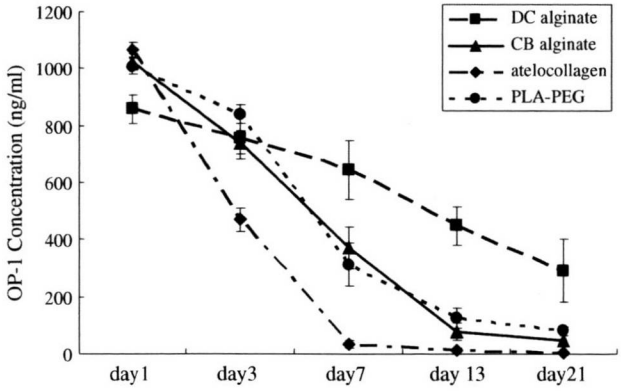

Fig. 3 OP-1 release from each carrier material/OP-1 (30 μg) composite was measured over time by a commercial BMP-7 ELISA kit. With each carrier material, the maximum concentration of OP-1 was detected on Day 1 and it decreased afterward. The decline was slowest in the DC alginate group.

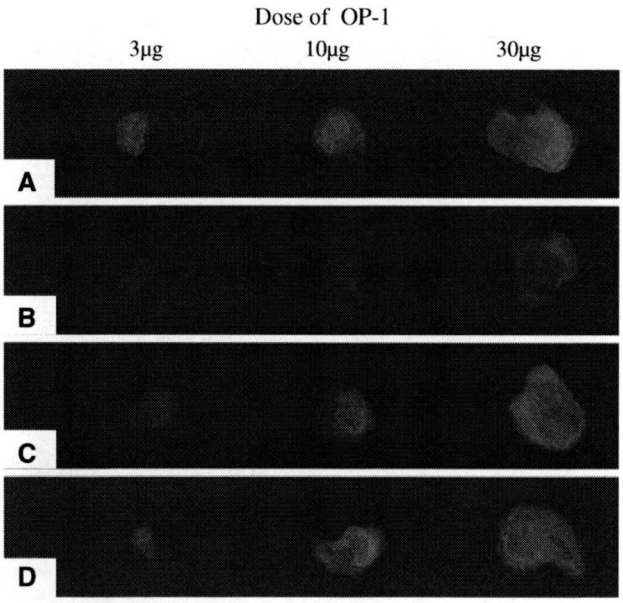

Fig. 4A–D The carriers for OP-1 tested were (**A**) DC alginate, (**B**) CB alginate, (**C**) atelocollagen, and (**D**) PLA-PEG. Soft xray photographs of ectopic bone induced by OP-1 (3, 10, or 30 μg) show bone formation with the DC alginate/OP-1 composite is equivalent or superior to that induced by the other carrier/OP-1 composites.

surrounding cancellous bone that contained hematopoietic bone marrow, and no inflammatory change was observed (Fig. 5A–D). These additional results were compatible with the results of BMC and ALP activity, suggesting that DC alginate can be an equivalent or superior carrier for a low dose of OP-1 compared with atelocollagen and PLA-PEG.

Discussion

Various materials have already been evaluated as carriers for BMPs, but they all have some disadvantages as mentioned previously. This study was designed to examine whether alginate, a material with no animal product content, is an equivalent or superior carrier for OP-1(BMP-7) compared with atelocollagen and PLA-PEG. Specifically we hypothesized: (1) BMC of bone nodules ectopically induced by DC alginate/OP-1 composite and/or CB alginate/OP-1 composite are equivalent or superior to those by atelocollagen and PLA-PEG; (2) ALP activity of bone nodules ectopically induced by DC alginate/OP-1 composite and/or CB alginate/OP-1 composite are equivalent or superior to those by atelocollagen and PLA-PEG; and (3) DC alginate and/or CB alginate have appropriate in vitro release kinetics of OP-1 equivalent to atelocollagen and PLA-PEG.

This study has several limitations. First, DC alginate was originally approved for clinical use as a cutaneous wound dressing [8, 37]. Therefore, its biodegradability and immunogenicity are unclear during use at a deeper site. Second, in the histological examination, DC alginate remained at the center of the new ectopic bone, indicating it had not degraded within 3 weeks. Although no inflammatory reaction was found, longer observation will be necessary before this material can be used with confidence at deeper sites. Third, ALP activity is a marker for osteoblastic differentiation, and is high in the early stage of osteoblast lineage. ALP activity is not necessarily parallel to the activity of bone formation. Fourth, in the release study, a commercial BMP-7 ELISA kit can only detect the amount of BMP-7(OP-1) protein, but cannot evaluate the activity of OP-1. The result of a release test may not reflect the actual activity of OP-1 released from carriers in vivo.

To determine whether DC alginate and/or CB alginate are equivalent or superior carriers for OP-1 compared with atelocollagen and PLA-PEG, we measured BMC of ectopic bone nodules as a primary research question. A previous study [24] reported that BMC of the ectopic bone induced by PLA-PEG/BMP-2 composite is about 6 mg higher than that by atelocollagen/BMP-2 composite. In our study, the BMC of DC alginate/OP-1 (3 μg) composite was about 6 mg higher than that of the atelocollagen/OP-1 (3 μg) composite and even much higher than that of CB alginate and PLA-PEG. The result of BMC measurement suggested that DC alginate is a highly effective carrier that enhances the bone-inducing effect of OP-1 even when OP-1 content is low.

The result of ALP activity measurement was compatible with the result of BMC, which reinforced the hypothesis that DC alginate is an equivalent or superior carrier compared with the other materials. Upon histological examination, not only trabecular bone but also normal hematopoietic bone marrow was observed, and we found

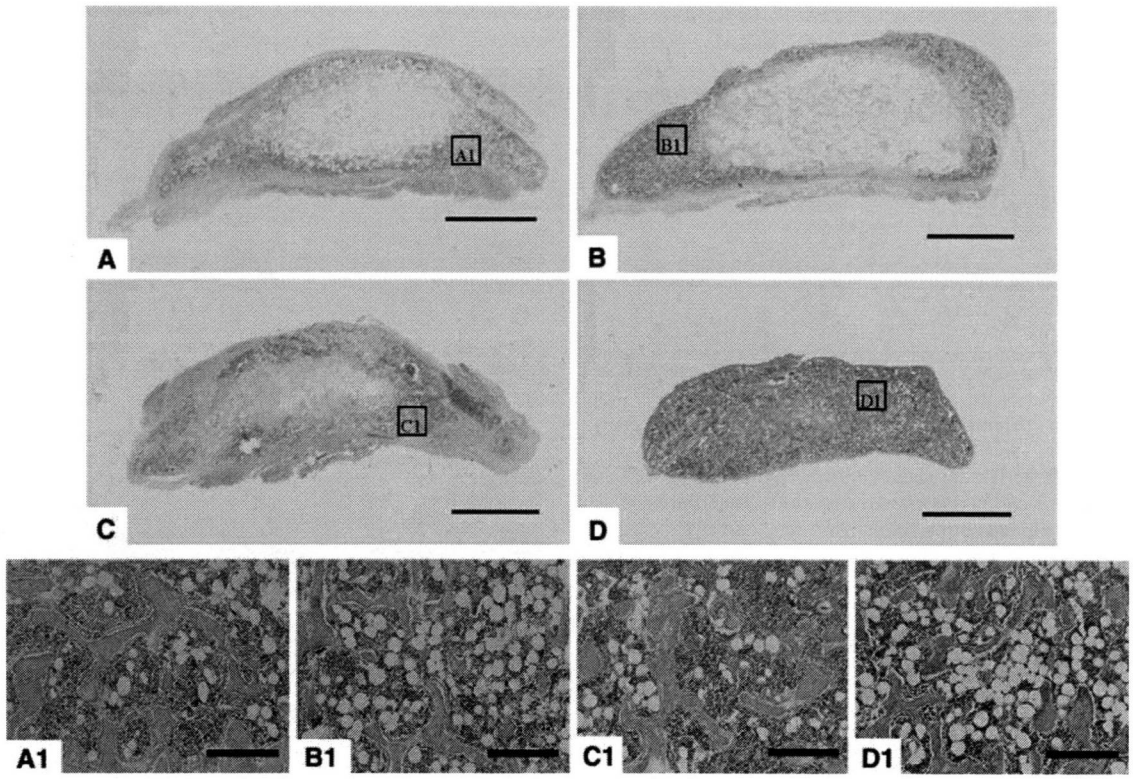

Fig. 5A–D Representative photomicrographs of the ectopic bone formation induced by OP-1 (30 μg) are shown (**A**, A1: DC alginate; **B**, B1: CB alginate; **C**, C1: atelocollagen; **D**, D1: PLA-PEG) (**A–D**: stain, hematoxylin and eosin; original magnification, ×10; scale bar = 2 mm; A1–D1: stain, hematoxylin and eosin; original magnification, ×100; scale bar = 200 μm). Irrespective of the carrier material, the newly formed bone had a thin cortex surrounding cancellous bone that contained highly cellular bone marrow.

no accumulation of inflammatory cells, such as monocyte/macrophages. The histological appearance of the ectopic bone induced by DC alginate/OP-1 composite seemed similar to that by atelocollagen/OP-1 composite, which is considered a safe biomaterial in terms of immunological response. These data suggested that DC alginate appears likely a safe material with no inflammatory response even when used in a deep site.

In contrast, CB alginate achieved relatively poor bone formation, especially with a low dose of OP-1. DC alginate and CB alginate only differ in the mode of crosslinking, but the release of OP-1 from these two alginates was quite different. It is known crosslinking by divalent cations forms a characteristic egg box structure that is suitable for trapping proteins in alginate [9]. Thus, the difference of bone formation between these two types of alginate may be partly due to a difference in their ability to retain OP-1 and release it slowly. It is also known the number of carboxyl residues in DC alginate is larger than that in CB alginate. The carboxyl residues induce apatite nucleation followed by the deposition of hydroxyapatite crystals on the alginate [35]. Furthermore, the Ca^{2+} contained in DC alginate can be utilized for new calcified bone, which is an advantage compared with CB alginate.

In conclusion, our data suggest DC alginate, a material with no animal product content that is approved by the FDA and other authorities, is a safe and potent carrier for OP-1. It is of note that DC alginate strongly potentiates osteoinduction of OP-1 even at a low dose. Thus, its use may reduce the cost of OP-1-based bone regeneration therapy.

Acknowledgments We thank Stryker Biotech, Smith & Nephew, Koyo Sangyo Co, Ltd, Johnson & Johnson, and Taki Chemicals Co, Ltd, for kindly providing the chemicals and materials.

References

1. Bach FH, Fishman JA, Daniels N, Proimos J, Anderson B, Carpenter CB, Forrow L, Robson SC, Fineberg HV. Uncertainty in xenotransplantation: individual benefit versus collective risk. *Nature Med.* 1998;4:141–144.
2. Bonadio J, Smiley E, Patil P, Goldstein S. Localized, direct plasmid gene delivery in vivo: prolonged therapy results in reproducible tissue regeneration. *Nature Med.* 1999;5:753–759.
3. Burkus JK, Dorchak JD, Sanders DL. Radiographic assessment of interbody fusion using recombinant human bone morphogenetic protein type 2. *Spine.* 2003;28:372–377.
4. Butler D, Wadman M, Lehrman S, Schiermeier Q. Last chance to stop and think on risks of xenotransplants. *Nature.* 1998;391:320–324.

5. Delustro F, Dasch J, Keefe J, Ellingsworth L. Immune responses to allogeneic and xenogeneic implants of collagen and collagen derivatives. *Clin Orthop Relat Res.* 1990;260: 263–279.
6. Einhorn TA. Enhancement of Fracture-Healing. *J Bone Joint Surg Am.* 1995;77:940–956.
7. Fang J, Zhu YY, Smiley E, Bonadio J, Rouleau JP, Goldstein SA, McCauley LK, Davidson BL, Roessler BJ. Stimulation of new bone formation by direct transfer of osteogenic plasmid gene. *Proc Natl Acad Sci USA.* 1996;93:5753–5758.
8. Gensheimer D. A review of calcium alginate. *Ostomy Wound Manage.* 1993;39:34–38, 42–43.
9. George M, Abraham TE. Polyionic hydrocolloids for the intestinal delivery of protein drugs: alginate and chitosan—a review. *J Controlled Release.* 2006;114:1–14.
10. Goldberg VM, Stevenson S. Natural history of Autografts and Allografts. *Clin Orthop Relat Res.* 1987;225:7–16.
11. Greesink RG, Hoefnagels NH, Bulstra SK. Osteogenic activity of OP-1 bone morphogenetic protein (BMP-7) in a human fibular defect. *J Bone Joint Surg Br.* 1999;81:710–718.
12. Jarque CM, Bera AK. Efficient tests for normality, homoscedasticity and serial independence of regression residuals. *Economics Letters.* 1980;6:255–259.
13. Johnsson R, Stromqvist B, Aspenberg P. Randomized radiostereometric study comparing osteogenic protein-1 (BMP-7) and autograft bone in human noninstrumented posterolateral lumbar fusion. *Spine.* 2002;27:2654–2661.
14. Kato M, Namikawa T, Terai H, Hoshino M, Miyamoto S, Takaoka K. Ectopic bone formation in mice associated with a lactic acid/dioxanone/ethylene glycol copolymer-tricalcium phosphate composite with added recombinant human bone morphogenetic protein-2. *Biomaterials.* 2006;27:3927–3933.
15. Kato M, Toyoda H, Namikawa T, Hoshino M, Terai H, Miyamoto S, Takaoka K. Optimized use of biodegradable polymer as a carrier material for the local delivery of recombinant human bone morphogenetic protein-2 (rhBMP-2). *Biomaterials.* 2006;27:2035–2041.
16. Kirker-Head CA. Potential applications and delivery strategies for bone morphogenetic proteins. *Adv Drug Deliv Rev.* 2000;43: 65–92.
17. Lee DD, Tofighi A, Aiolova M, Chakravarthy P, Catalano A, Majahad A, Knaack D. Alpha-BSM: a biomimetic bone substitute and drug delivery vehicle. *Clin Orthop Relat Res.* 1999;367: S396–S405.
18. Matsumine A, Myoui A, Kusuzaki K, Araki N, Seto M, Yoshikawa H, Uchida A. Calcium hydroxyapatite ceramic implants in bone tumor surgery: a long-term follow-up study. *J Bone Joint Surg Br.* 2004;86:719–725.
19. Miyamoto S, Takaoka K, Okada T, Yoshikawa H, Hashimoto J, Suzuki S, Ono K. Evaluation of polylactic acid homopolymers as carriers for bone morphogenetic protein. *Clin Orthop Relat Res.* 1992;278:274–285.
20. Miyamoto S, Takaoka K, Okada T, Yoshikawa H, Hashimoto J, Suzuki S, Ono K. Polylactic acid-polyethylene glycol block copolymer: a new biodegradable synthetic carrier for bone morphogenetic protein. *Clin Orthop Relat Res.* 1993;294:333–343.
21. Nemzek JA, Arnoczky SP, Swenson CL. Retroviral transmission by the transplantation of connective-tissue allografts. *J Bone Joint Surg Am.* 1994;76:1036–1041.
22. Ohgushi H, Dohi Y, Toshikawa T, Tamai S, Tabata S, Suwa Y. In vitro bone formation by rat marrow cell culture. *J Biomed Mater Res.* 1996;32:341–348.
23. Saito N, Murakami N, Takahashi J, Horiuchi H, Ota H, Kato H, Okada T, Nozaki K, Takaoka K. Synthetic biodegradable polymers as drug delivery systems for bone morphogenetic proteins. *Adv Drug Deliv Rev.* 2005;57:1037–1048.
24. Saito N, Okada T, Horiuchi H, Murakami N, Takahashi J, Nawata M, Ota H, Miyamoto S, Nozaki K, Takaoka K. Biodegradable poly-D,L-lactic acid-polyethylene glycol block copolymers as a BMP delivery system for inducing bone. *J Bone Joint Surg Am.* 2001;83 Suppl 1(Pt 2):S92–S98.
25. Saito N, Okada T, Horiuchi H, Ota H, Takahashi J, Murakami N, Nawata M, Kojima S, Nozaki K, Takaoka K. Local bone formation by injection of recombinant human bone morphogenetic protein-2 contained in polymer carriers. *Bone.* 2003;32:381–386.
26. Saito N, Okada T, Toba S, Miyamoto S, Takaoka K. New synthetic absorbable polymers as BMP carriers: plastic properties of poly-D,L-lactic acid-polyethylene glycol block copolymers. *J Biomed Mater Res.* 1999;47:104–110.
27. Saito N, Takaoka K. New synthetic biodegradable polymers as BMP carriers for bone tissue engineering. *Biomaterial.* 2003;24: 2287–2293.
28. Schmidmaier G, Schwabe P, Strobel C, Wiidemann B. Carrier systems and application of growth factors in orthopaedics. *Injury.* 2008; 39 Suppl 2:S37–43.
29. Seeherman H, Wozney J M. Delivery of bone morphogenetic proteins for orthopedic tissue regeneration. *Cytokine Growth Factor Rev.* 2005;16:329–345.
30. Suzuki Y, Tanihara M, Nishimura Y, Suzuki K, Yamawaki Y, Kudo H, Kakimaru Y, Shimizu Y. In vivo evaluation of a novel alginate dressing. *J Biomed Mater Res.* 1999;48:522–527.
31. Takaoka K, Koezuka M, Nakamura H. Telopeptide-depleted bovine skin collagen as a carrier for bone morphogenetic protein. *J Orthop Res.* 1991;9:902–907.
32. Takaoka K, Nakahara H, Yoshikawa H, Masuhara K, Tsuda T, Ono K. Ectopic bone induction on and in porous hydroxyapatite combined with collagen and bone morphogenetic protein. *Clin Orthop Relat Res.* 1988;234:250–254.
33. Tamai N, Myoui A, Tomita T, Nakase T, Tanaka J, Ochi T, Yoshikawa H. Novel hydroxyapatite ceramics with an interconnective porous structure exhibit superior osteoconduction in vivo. *J Biomed Mater Res.* 2002;59:110–117.
34. Tamura S, Kataoka H, Matsui Y, Shionoya Y, Ohno K, Michi KI, Takahashi K, Yamaguchi A. The effects of transplantation of osteoblastic cells with bone morphogenetic protein (BMP)/carrier complex on bone repair. *Bone.* 2001;29:169–175.
35. Tanahashi M, Matsuda T. Surface functional group dependence on apatite formation on self-assembled monolayers in a simulated body fluid. *J Biomed Mater Res.* 1997;34:305–315.
36. Urist MR. Bone formation by autoinduction. *Science.* 1965;150: 893–899.
37. Vanstraelen P. Comparison of calcium sodium alginate (KALTOSTAT) and porcine xenograft (E-Z DERM) in the healing of split-thickness skin graft donor sites. *Burns.* 1992;18:145–148.
38. Wang EA, Rosen V, D'Alessandro JS, Baudny M, Cordes P, Harada T, Israel DI, Hewick RM, Kerns KM, LaPan P, Luxenberg DP, McQuaid D, Moutsatsos IK, Nove J, Wozeny EA. Recombinant human bone morphogenetic protein induces bone formation. *Proc Natl Acad Sci USA.* 1990;87:2220–2224.

Journal of Clinical Pharmacy and Therapeutics (2009) **34**, 355–361 doi:10.1111/j.1365-2710.2009.01046.x

PHARMACOGENETICS

Genetic polymorphisms in folate pathway enzymes as a possible marker for predicting the outcome of methotrexate therapy in Japanese patients with rheumatoid arthritis

H. Hayashi* MSc, C. Fujimaki* BS, T. Daimon† PhD, S. Tsuboi‡ MD, T. Matsuyama§ BS and K. Itoh* PhD

**Department of Clinical Pharmacology & Genetics, †Department of Drug Evaluation & Informatics, School of Pharmaceutical Sciences, University of Shizuoka, ‡Department of Rheumatology and §Department of Pharmacy, Shizuoka Kousei Hospital, Shizuoka, Japan*

SUMMARY

Background: **Low-dose methotrexate (MTX) therapy is widely used in the treatment of rheumatoid arthritis (RA). Though the difference in response to MTX between patients with RA is large, the factors that contribute to this variability remain unclear.**

Objective: **We aimed to identify those factors with a particular emphasis on the pharmacogenetics of MTX.**

Method: **We evaluated the association of possible factors, including genetic polymorphisms of folate metabolic pathway enzymes, with the cumulative value of C-reactive protein, an index of MTX anti-inflammatory efficacy, in 87 Japanese patients with RA.**

Results: **Polymorphisms of the reduced folate carrier gene (*RFC*) G80A and of the γ-glutamylhydrolase gene (*GGH*) C−401T were more closely associated (β = 2·1194, *P* = 0·0017) than other polymorphisms, with the anti-inflammatory response to MTX.**

Conclusion: **Patients with RA having *RFC* 80A and *GGH* −401T alleles were less responsive to MTX than those with *RFC* 80A and without *GGH* −401T alleles. Thus, this data may be useful for guiding treatment of RA patients with MTX.**

Received 13 April 2008, Accepted 25 July 2008
Correspondence: K. Itoh, PhD, Professor, Department of Clinical Pharmacology & Genetics, School of Pharmaceutical Sciences, University of Shizuoka, 52-1 Yada, Suruga-ku, Shizuoka 422-8526, Japan. Tel.: +81 54 264 5673; fax: +81 54 264 5673; e-mail: itohk@u-shizuoka-ken.ac.jp

***Keywords*: C-reactive protein, γ-glutamylhydrolase, methotrexate, polymorphism, reduced folate carrier, rheumatoid arthritis**

INTRODUCTION

Methotrexate (MTX) is an antifolate that is widely used to treat hyper-immune disorders [e.g., rheumatoid arthritis (RA), and cancers, including childhood acute lymphoblastic leukemia] (1–6). In general, low-dose MTX, usually administered orally as a weekly pulse, is first-line therapy for RA that is unresponsive to non-steroidal anti-inflammatory drugs (7); however, it is associated with over-immunosuppression, which may lead to bone marrow depression and increased susceptibility to infection (8). Though the response to low-dose MTX shows wide inter-patient variability (9–11), the contributing factors remain unclear. However, the differences in dosage requirement are usually attributed to inter-patient differences in pharmacokinetics and pharmacodynamics parameters.

Intestinal absorption of MTX and its uptake into target cells are mainly controlled by the polymorphic reduced folate carrier gene (*RFC*). A previous report demonstrated that in patients with leukemia treated with MTX, a single nucleotide polymorphism (SNP) G80A was associated with higher MTX concentration (12). However, a recent study reported that *RFC* G80A SNP affects MTX treatment outcome in RA (13) and that remission of RA symptoms was significantly higher in *RFC* 80AA carriers in comparison with 80GG individuals (odds ratio = 3·32).

After cell entry, MTX is rapidly converted to γ-glutamyl polyglutamates (PGs) by folylpolyglutamate synthetase, which sequentially adds up to six glutamyl residues to MTX (14–16). MTX-PGs are potent inhibitors of dihydrofolate reductase (DHFR) resulting in depletion of reduced folates, the cofactors for thymidylate synthase (17). γ-Glutamyl hydrolase (GGH) is a lysosomal peptidase that catalyses the removal of γ-linked polyglutamates, converting long-chain MTX-PGs into short-chain MTX-PGs and ultimately to MTX, allowing folate to be exported from the cell (18, 19). Several SNPs have been identified in the *GGH* gene (e.g., C–401T, G–354T, and C452T) (20). Cheng *et al.* reported that *GGH* C452T (Thr127Ile) significantly reduced the activity of GGH in hydrolyzing long-chain MTX-PGs, and led to MTX-PGs accumulation in acute lymphoblastic leukemia blasts of patients treated with high-dose MTX (21). Allele frequency in this SNP vary significantly between different ethnic groups and we reported the genotype distribution and allele frequency of *GGH* C452T in a Japanese population (22). All of the promoter polymorphisms analyzed enhanced GGH expression (20). *GGH* C–401T has been shown to be associated with altered accumulation of MTX-PGs in RA patients treated with MTX (23).

Methylenetetrahydrofolate reductase (MTHFR) has a critical role in the folate cycle. It converts 5,10-methylene-tetrahydrofolate (methyl-donor in thymidine monophosphate synthesis) to 5-methyltetrahydrofolate (carbon donor required for methionine synthesis). Moreover, two common SNPs in the *MTHFR* gene (C677T and A1298C) have been found to influence the efficacy and toxicity of MTX (24, 25).

Current MTX dosing algorithms do not include the genetic background of patients with RA, although it could affect the response to MTX. Thus, the aim of this study was to examine what factors, including SNPs of these genes, were associated with the anti-inflammatory response to low-dose MTX therapy in Japanese patients with RA.

MATERIALS AND METHODS

Patients

We recruited 219 patients with RA in our study from the Department of Rheumatology, Shizuoka Kousei Hospital. RA was diagnosed according to American College of Rheumatology criteria. Eighty-seven patients who had been receiving weekly pulse of MTX for ≥12 months, and were undergoing analysis of blood biochemistry at least every 2 months during the previous 12 months, were selected. Patients receiving concurrent therapy known to affect MTX dosing (e.g., infliximab, etanercept, tacrolimus, cyclosporine) were excluded. Written informed consent was obtained from all patients after a detailed briefing of the purpose and protocol of the study. Age, sex, body weight, additional medical problems, and concurrent medications were recorded. A blood sample was taken for serum C-reactive protein (CRP) and creatinine measurement and *RFC*, *GGH* and *MTHFR* genotyping. We used the CRP level as a marker of inflammatory status in RA because CRP is highly sensitive in this respect, and is not affected by sex, age, or other proteins. The area under the curve of the serial CRP measurements (CRP-AUC) was calculated to quantify total inflammatory status during 12 months of MTX treatment. CRP-AUC is associated with the outcome of RA treatment (26, 27). Creatinine clearance was calculated according to the Cockcroft–Gault formula (28). Glucocorticoids doses were calculated as prednisolone-equivalent doses, where 5 mg prednisolone was equivalent to 20 mg hydrocortisone, 750 μg dexamethasone, or 750 μg betamethasone (29). This study was approved by the Ethics Committee of Shizuoka Kousei Hospital and the University of Shizuoka.

Genotyping assays

Leukocyte genomic DNA was extracted directly from whole blood using a QIAamp DNA Blood Mini Kit (Qiagen, Hilden, Germany). Genotyping was performed using polymerase chain reaction–restriction fragment length polymorphism (PCR–RFLP) and allele-specific PCR (AS-PCR) assays. Primer sequences, PCR conditions and restriction enzymes are shown in Table 1. PCR products and restriction enzyme digestion products were electrophoresed on 2–4% agarose gels with ethidium bromide and viewed under UV light.

Data analyses

To identify factors associated with CRP-AUC, the data were analyzed with respect to age, sex, body

